

Spontaneous Atomic Ordering in Semiconductor Alloys: Causes, Carriers, and Consequences

Alex Zunger

MRS
BULLETIN
REPRINT

Reprinted from Materials Research Society
MRS Bulletin, Volume 22, Number 7,
July 1997

Spontaneous Atomic Ordering in Semiconductor Alloys: Causes, Carriers, and Consequences

Alex Zunger

Introduction

For many years, it was believed that when two isovalent semiconductors are mixed, they will phase-separate (like oil and water) at low temperature, they will form a solid solution (like gin and tonic) at high temperatures, but they will never produce ordered atomic arrangements. This view was based¹⁻³ on the analysis of the solid-liquid equilibria at high temperatures and on empirical observation of phase separation at low temperatures. These observations were further rationalized and legitimized by applying the classic (Hildebrand) solution models, which predicted just this type of behavior. These models showed that the observed behavior of the A_xB_{1-x} alloys implied a *positive* excess enthalpy $\Delta H(x) = E(x) - xE(A) - (1-x)E(B)$ (where E is the total energy) and that this positiveness (“repulsive A-B interactions”) resulted from the strain energy³ attendant upon packing two solids with dissimilar lattice constants. The larger the lattice mismatch, the more difficult it was to form the alloy.³ Common to these approaches (“regular solution theory,” “quasiregular solution theory,” “delta lattice-parameter model,” etc.) was the assumption that the enthalpy $\Delta H(x)$ of an alloy depends on its global composition x but not on the microscopic arrangement of atoms (e.g., ordered versus disordered). Thus, ordered and disordered configurations at the same compo-

sition x were tacitly assumed to have the same excess enthalpy $\Delta H(x)$. Clearly the option for ordering was eliminated at the outset. While these theories served to produce very useful depictions of the immiscibility of many semiconductor alloys (and continue to guide strategies of crystal growth), they also cemented the paradigm that semiconductor alloys don’t order, they just phase-separate. This was true, at the time.

When I approached this problem in early 1984, one glaring exception to the accepted paradigm stood out: Despite a huge (~40%) lattice-constant mismatch between diamond and silicon, the isovalent alloy Si_xC_{1-x} was known to order crystallographically at $x = 0.5$ (much like Cu and Au). In this system, the excess enthalpy of the ordered phase $\Delta H(\text{ordered})$ was *negative*.⁴ In contrast, we knew that III-V alloys behaved differently, having positive $\Delta H(x) > 0$, at least for the random phase. While Hume-Rothery knew already four decades ago that when $\Delta H(x) < 0$ (which is the case in “compound-forming systems,” such as Cu-Au or Si-C), size differences can lead both to short- and to long-range order, in compound semiconductors, we were faced with a completely different situation: $\Delta H(x)$ was *known* to be positive, so Hume-Rothery’s ideas did not apply. Could a system with $\Delta H(\text{random}, x) > 0$ order crystallographically?

When Srivastava, Martins, and I⁵ looked into the problem, we found theoretically that ordered and disordered atomic configurations of III-V alloys at the same composition x could have very different enthalpies—in principle, even different signs of $\Delta H(x)$, a situation that is extremely rare in metallurgy. Thus we predicted⁵ that even though it was not observed at the time, long-range atomic ordering in III-V alloys was in principle possible *despite* $\Delta H(\text{random}) > 0$. A detailed phase-diagram calculation illustrating coexistence of ordering and phase separation followed.⁶ The reason that $\Delta H(\text{ordered}) < 0$ could coexist with $\Delta H(\text{random}) > 0$ [or at least that $0 < \Delta H(\text{ordered}) < \Delta H(\text{random})$] was^{4,5} that certain *ordered* three-dimensional (3D) atomic arrangements minimize the strain energy resulting from the large lattice-constant mismatch between the constituents, while random arrangements do not. Clearly the key was that in strained systems, different atomic arrangements could have very different enthalpies at the same composition.

After our paper (Reference 5) was received by *Physical Review*, I visited the IBM T.J. Watson Research Laboratory. T. Kuan stood up after the seminar I gave, and said that he had just observed ordering in $Al_xGa_{1-x}As$ alloys and was planning to submit a paper soon.⁷ (Ironically the ordering in the lattice-matched $Al_xGa_{1-x}As$ system is still the least understood case.) Soon after, many other sightings of spontaneous ordering in III-V alloys were reported—for example, by Nakayama and Fujita⁸ (liquid-phase epitaxy [LPE]—InGaAs), by Jen et al.⁹ (metalorganic chemical vapor deposition [MOCVD]—GaAsSb), by Shahid et al.¹⁰ (vapor levitation epitaxy—InGaAs), and by Gomyo et al.^{11,12} (MOCVD—GaInP and molecular-beam epitaxy—AlInAs). An INSPEC® literature search shows that at the time this article was written, over 700 articles dealing with spontaneous ordering in semiconductor alloys were published. What we have learned in the intervening years from these many experimental studies is that the minimization of strain by the ordered atomic patterns, which we have originally envisioned to occur in bulk systems,⁵ was actually greatly enhanced by the existence of a free surface nearby. I’ll describe this important realization in the next section. In it, you will see that ordered atomic arrangements correspond to the *thermodynamically stable structure* for a few monolayers near the surface. Yet deeper into the film, the thermodynamically stable structure reverts to either phase

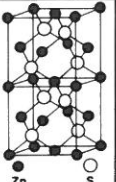
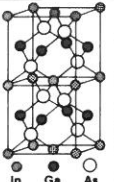
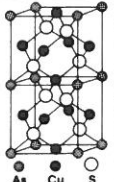
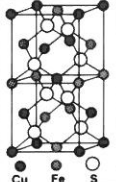
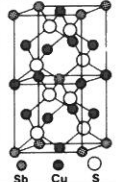
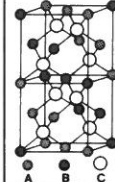
Ordering Vectors	(0,0,0)	(0,0,1)		(2,0,1)		(1,1,1)
Name (ternary)	Zinc Blende (Sphalerite)	Layered Tetragonal	"Luzonite"	Chalcopyrite	Famatinite	Layered Trigonal
Formula:	$n = 0,4; AC$	$n = 2; ABC_2$	$n = 1,3; A_3BC_4$	$n = 2; ABC_2$	$n = 1,3; A_3BC_4$	$n = 2; ABC_2$
						
Example: (ternary)	ZnS-type	InGaAs ₂ -type	Cu ₃ AsS ₄ -type	CuFeS ₂ -type	Cu ₃ SbS ₄ -type	CrCuS ₂ -type (Na V S ₂)

Figure 1. The crystal-structure forms of ordered isovalent semiconductor alloys. The last structure is layered trigonal "CuPt."

separation¹³ (if the film is incoherent) or to chalcopyrite ordering^{5,14} (if it is coherent). Thus for the surface-stabilized *ordered* structure to propagate deep into the film (in preference to phase separation or chalcopyrite ordering), one needs to assume that once covered by a few monolayers of incoming atoms, the ordered structure is "frozen in." Thus while the *cause* of near-surface ordering is thermodynamic, its carrier into the interior of the film is controlled by growth kinetics. Since the failure to delineate between the *causes* of ordering and the mechanism for its *propagation* into the film have led to much confusion in the literature, I will discuss them separately in the following. I will then describe the main consequences of ordering on materials properties, emphasizing yet untested theoretical predictions that could provide interesting research opportunities.

The Cause of Atomic Ordering (Surface Thermodynamics)

One's first, common-sense step in trying to assess the stability or instability of ordered compounds is to inspect the *formation enthalpy of periodic, bulk structures*:

$$\Delta H(\text{ordered}, \sigma) = E(\text{ordered}, \sigma) - xE(A) - (1-x)E(B). \quad (1)$$

Here $E(\text{ordered}, \sigma)$ is the total energy of a given arrangement σ ("configuration") of A and B atoms on a lattice with N sites, $x = N_B/N$ and $E(A)$ and $E(B)$ being the total energies of the constituent solids.

Accurate, first-principles local-density approximation calculations^{4-6,13,14} for many pseudobinary semiconductors in the leading bulk structures (Figure 1) have revealed that $\Delta H(\text{ordered}, \sigma) > 0$ for all, except SiC in the zinc-blende

structure⁴ and AlInX_2 in the chalcopyrite structure¹⁴ (with $X = \text{P, As}$), for which *stable bulk ordering* $\Delta H(\text{ordered}, \sigma) < 0$ was predicted. However the often observed¹¹ layered trigonal CuPt ordered structure (Figure 1) was found to have the *highest* formation energy of all high-symmetry, ordered bulk structures. This implies that the ground state of periodic, isovalent bulk $A_xB_{1-x}C$ semiconductor alloys is generally phase separation into $(x)AC + (1-x)BC$. One could wonder whether in this approach of inspecting just a few (Figure 1) structures ("rounding up the usual suspects"?), stable but uncommon atomic configuration might have been overlooked. However a special technique called "ground-state search of cluster-expanded energies"¹³ permits one to expand $\Delta H(\text{ordered}, \sigma)$ for *any* of the 2^N configurations σ in a series of many-body atom-atom interactions and search this (astronomically large) configurational space via "simulated-annealing" techniques. In this case, the result was¹³ that for pseudobinary III-V semiconductor alloys, no new stable bulk ordered structures were found.

Interestingly however, while generally $\Delta H(\text{ordered}, \sigma) > 0$, we did identify some special (s) ordered structures $\{\sigma_s\}$ that have the lower energies at the composition x_σ . In particular they have lower energies than the random alloy of the same composition—that is, $\Delta H(\text{ordered}, \sigma_s) < \Delta H(\text{random } x)$, where the mixing enthalpy of the random alloy is

$$\Delta H(\text{random}, x) = E(\text{random}, x) - xE(A) - (1-x)E(B). \quad (2)$$

For alloys of diamondlike components (Si-Ge), σ_s is the rhombohedral "RH1" structure⁴ and the zinc-blende structure. For alloys of III-V or II-VI zinc-blende

components, σ_s is the ABC_2 chalcopyrite structure^{6,13,14} or the A_3BC_4 famatinite ("DO₂₂-like") structure.¹³ For alloys whose components have the rock salt structure (e.g., PbS, PbSe, PbTe), σ_s has the (octahedral) CuPt structure (Table I).

What is special about these 3D configurations? It turns out that some of them (e.g., RH1) have a very unique topological property—they possess just enough structural degrees of freedom to accommodate *any* (in particular, "ideal") bond length and bond angle. Thus of all 2^N possible configurations, the structures of Table I are the lowest strain energy configurations in the adamantite family.

The identification of these special structures had two implications. *First* it meant that the bulk *random alloy* could lower its energy by developing *short-range order* ("anti-clustering"¹³) of the specific form that mimics the local atomic arrangements in the "special structures" $\{\sigma_s\}$. This prediction awaits experimental testing (e.g., via x-ray diffuse scattering). *Second* if bulk phase separation were to be inhibited (e.g., by coherency strain), the alloy could develop *long-range order* in crystal structures shown in Table I. These predictions too await experimental testing.

Having found that long-range *bulk* ordering of pseudobinary semiconductor alloys is generally not the thermodynamically preferred structure at conventional growth temperatures, we next considered nonbulk structures. Specifically we were wondering whether it was possible that the thermodynamically stable atomic arrangement near a surface will be qualitatively different from the thermodynamically stable arrangement in an infinite bulk solid. That the surface has an important role in ordering was already clear from the experimentally observed fact¹¹ that of the four bulk-equivalent {111} directions, ordering is usually observed only along two of them ("CuPt_B variants") while the other two ("CuPt_A") are missing, at least when grown on a (2×4) surface, but how specifically does a surface intervene? Does it create an atomic configuration that does not correspond to a minimum in the surface free energy but is instead a kinetic transient trapped in by the growth process ("kinetic ordering"), or does the surface create a new minimum in the free energy corresponding to a stable atomic structure there ("thermodynamic ordering")?

Our strategy was to test the second possibility and to appeal to the first possibility only if the former failed. To this end, we have performed extensive first-

principles total energy calculations for various assumed surface reconstructions of $\text{Ga}_x\text{In}_{1-x}\text{P}/\text{GaAs}(001)$, contrasting the energies of many atomic configurations.¹⁵⁻¹⁷ Such calculations are considerably more involved than previous first-principles calculations on the surface structures of *pure* (nonalloyed) compounds (e.g., GaAs), as now the statistical alloy degrees of freedom had to be treated. Just as we had envisioned that certain ordered atomic arrangements minimize the strain energy in the 3D bulk⁵ (Table I), so do certain atomic arrangements minimize the total energy at a few subsurface layers below a reconstructed surface (Table II). There were however two significant differences between the bulk structures and the near-surface structures: *First* the symmetries of the minimum-energy configurations near a surface (CuPt and the “three period superlattices”) are different from those of the minimum energy configurations in a 3D bulk material (chalcopyrite). *Second*, near a surface, the

special ordered arrangements (Table II) are stabler than even phase separation, so they are predicted to be the *absolute* thermodynamic ground states there. In the bulk on the other hand, the special structures (Table I) are stabler than the random alloy, but in many cases they are metastable with respect to phase separation.

What is special about these near-surface configurations? The answer appears on the cover of this issue. The upper panel shows a $\beta 2(2 \times 4)$ reconstructed surface of $\text{Ga}_{0.5}\text{In}_{0.5}\text{P}$ (which is believed to be the stable reconstruction of anion-stabilized III-Vs). This reconstruction¹⁷ contains three P-P dimers per surface unit cell: two upper dimers and a lower dimer. It corresponds to 3/4 anion coverage. Thus the surface has a “missing dimer row.” The first subsurface layer (marked $h = 1$) contains four threefold (labeled “3”) and two fourfold (labeled “4”) coordinated cations. The second subsurface layer ($h = 2$) contains only P atoms. The third subsurface layer ($h = 3$) contains four symmetry-distinct

cation sites, labeled A, B, C, and D. The A and B sites lie directly *under* the top surface P-P dimer, so they are compressed. The C and D sites lie under the “missing dimer row,” so they are under tension. We see that *the existence of surface dimers breaks the symmetry among the bulk-equivalent cation sites A, B, C, and D*. Our total energy calculations¹⁶⁻¹⁸ started from a pure InP(001) surface and gradually increased the Ga content (under P-stabilized conditions), determining the chemical potential $\Delta\mu = \mu_{\text{Ga}} - \mu_{\text{In}}$ at which each cation site (“3,” “4,” A, B, C, D) in the film will prefer to switch its occupation from In to Ga. The results show that because sites A and B are under *compression*, they immediately prefer to be occupied by the *small cation* (Ga), while sites C and D, being under *tension*, remain occupied by the *large cation* (In) even until $\Delta\mu$ was quite high. The two-dimensional (2D) atomic configuration resulting from this atomic occupation pattern is consistent with the CuPt_B structure, with a planar ordering direction $[\bar{1}10]$, which is the dimer orientation. The penalty for making an “occupation error”—for example, occupying site B by In and site C by Ga—is quite high: ~ 150 meV/atom. Thus surface reconstruction exerts a significant ordering-promoting configurational selectivity in subsurface layers.

This subsurface selectivity induced by the dimers on the top surface naturally depends on the *dimer orientation*. In a $c(4 \times 4)$ reconstructed surface (lower panel on the cover of this issue), the surface is terminated by one and three-quarters monolayers of P, so the dimer row is now 90° rotated with respect to the 3/4 coverage in the $\beta 2(2 \times 4)$ case, being now along $[110]$. The $h = 2$ (second subsurface) layer has three types of fourfold coordinated cation sites: A and B being under the dimer, and C being under a missing dimer row. As before, the compressed A and B sites prefer occupation by the smaller Ga, while site C stays occupied by In until $\Delta\mu$ reaches a large value. The ensuing structure is consistent with CuPt_A , with a planar ordering direction $[110]$, which is the dimer direction in this surface. The ordering energy is 155 meV/atom. Similar calculations¹⁵⁻¹⁷ have shown that the cation-terminated (2×2) reconstruction drives CuPt_B ordering both at $h = 0$ and at $h = 4$, while $\beta 2(4 \times 2)$ drives CuPt_B ordering (ordering energy of ~ 100 meV/atom), and the recently predicted¹⁷ $c(8 \times 6)$ reconstruction drives a special, triple-period ordering at $h = 2$, with an ordering energy of 97 meV/atom. These results are summa-

Table I: Three-Dimensional Adamantine Structures That Minimize the Strain Energy Resulting From Atomic Size Mismatch.

Structure of Binary Constituents	Strain-Minimizing Ternary Structure
Diamondlike (Si, Ge)	RH1 and Zinc Blende ⁴
Zinc-Blende (InP, GaP)	Chalcopyrite and Faminite ^{13,14}
Rock-Salt (PbS, PbTe)	CuPt

Table II: Predicted Near-Surface Equilibrium Atomic Long-Range Order (in the h -th Subsurface Layer) and the Equilibrium Segregating Atom in Mixed Cation GaInP Alloys.¹⁵⁻¹⁸

Surface Reconstruction	Near-Surface Ordering	Segregation
(2×2) Cation-terminated	CuPt-B ($h = 0,4$)	In
$\beta 2(4 \times 2)$ Cation-terminated	CuPt-B ($h = 2$)	Ga
$\beta 2(2 \times 4)$ Anion-terminated (2×1) RHEED	CuPt-B ($h = 3$)	In
$c(4 \times 4)$ Anion-terminated (1×2) RHEED	CuPt-A ($h = 2$)	In
$c(8 \times 6)$ Anion-terminated (2×3) RHEED	3-period SL ($h = 2$)	?

RHEED = reflection high-energy electron diffraction.

rized in Table II. Simple thermodynamic models show that these large ordering energies yield¹⁷ a large (up to 60%) degree of ordering even at growth temperatures.

Ordering and Surface Segregation

The same type of calculation¹⁶ that predicts ordering can predict the type of surface segregation expected for each reconstruction and each subsurface layer. This is done by determining the occupation of each cation site (by Ga or In) at the chemical potential value $\Delta\mu_0$ that produces a given occupation (e.g., 50%–50%) in the bulk. If at $\mu = \Delta\mu_0$, the occupancy of layer h by Ga(In) exceeds the bulk value, we say that Ga(In) “segregates at layer h ” (Table II). The figure on the cover shows, for example, that the first subsurface layer ($h = 1$) in a $\beta 2(2 \times 4)$ surface of $\text{Ga}_{0.5}\text{In}_{0.5}\text{P}/\text{GaAs}$ (001) segregates pure In. Site “4” in that layer stays occupied by In longer than site “3.” Table II shows the predicted segregations for each reconstruction. Remarkably, different reconstructions of the same surface face (001) produce different segregations!

It is possible that this dependence of segregation on reconstruction could be used advantageously to grow abrupt interfaces: insofar as interfacial roughness is caused by segregation, it might be possible to “dial in” an In-segregating reconstruction $\beta 2(2 \times 4)$ during the growth of InAs-on-GaAs and a Ga-segregation reconstruction $\beta 2(4 \times 2)$ during the growth of GaAs-on-InAs. The surface segregation effect would then work to make both the In-on-Ga and the Ga-on-In interfaces abrupt. This suggestion awaits experimental testing.

We have thus seen that reconstruction-driven surface energetics stabilizes distinct subsurface ordering patterns and surface segregation patterns (Table II). Finite-temperature statistical-mechanics models^{16–17} based on these total energy calculations predict that ordering degrees of 30–60% are possible at typical growth temperatures. The predicted ordered structures indicated in Table II agree with those observed experimentally earlier in postgrowth transmission-electron-microscopy studies (e.g., see the review in Reference 18 and also References 11 and 12) for all reconstruction patterns noted in the table. No *in situ* scanning-tunneling-microscopy (STM) studies exist as yet to test the specific surface-ordering patterns predicted theoretically (cover and Table II). Such studies would be a natural extension into alloys from previous STM investigations of surfaces in pure zinc-blende compounds.

The Carrier of Atomic Ordering (Growth Kinetics)

Surface thermodynamics predicts the structures that surface atoms would like to attain (ordered patterns), but growth kinetics determines the extent to which this wish can come true during a particular growth experiment. Indeed, growth kinetics is the “carrier” or “propagator” of near-surface atomic ordering into the interior of the film. Thus parameters controlled during growth, such as rates, partial pressures, substrate misorientation, temperatures, V/III ratio, and the presence of fast-diffusing impurities, can and do affect the degree of ordering in a film.¹⁸ (Unfortunately such dependences were often misconstrued to imply that the growth effects are the causes of ordering rather than the propagators of ordering.)

Theoretical modeling of growth kinetics^{19–20} often assumes a thermodynamic driving force (e.g., stable surface ordering^{19–20}) and a series of kinetic obstacles (i.e., surface roughening, activated attachment/detachment/hopping of atoms). Such models teach us how the assumed obstacles (and the postulated obstacle parameters—i.e., activation energies) impede the propagation of ordering into the film. For example¹⁹ while a large ratio D/F between the atomic-diffusion constant (D) and the deposition rate (F) permits atoms to find their thermodynamically mandated (ordered) positions, a small D/F ratio leads to an increase in step density with a concomitant decrease in long-range order (A-B pairing) and an increase in short-range clustering (A-A and B-B pairing). Since long-range order is the thermodynamic ground state near the surface, any kinetic loss of order must raise the free energy and hence tends to smooth the surface roughness.¹⁹ Kinetics can also be the vehicle that propagates ordering. For example,¹⁸ step flow could position the thermodynamically ordered 2D layers at several height values h (cover), thus constructing a 3D stack.

At present it appears that semiconductor-alloy growth-simulation models are still at their early stages, as the relative roles and importance of the many different elementary growth events—step bunching, single-to-double step transitions, island formation due to strain relief, Schwabel barriers, faceting, activated atomic hopping and attachment events, and rippling instabilities—are still being sorted out. No first-principles (or even second-principles) theory of such events exists as yet. This is an important challenge to theory. The remarkable experimental work done in this field

by Gomyo and Suzuki, and by Stringfellow’s group (see articles by Suzuki and Stringfellow in this issue), appear to lead the theoretical studies at this time.

The Consequences of Atomic Ordering (Fingerprints)

Long-range ordering (LRO) of the CuPt type (Figure 1) is manifested by the existence of alternate cation-monolayer planes $A_{x+\eta/2}B_{1-x-\eta/2}$ and $A_{x-\eta/2}B_{1-x+\eta/2}$, stacked along the [111] (or equivalent) directions, where $0 \leq \eta \leq 1$ is the CuPt long-range order parameter. Perfect ordering ($\eta = 1$, $x = 1/2$) corresponds to successive planes of pure A followed by pure B, etc. Thermodynamic calculations of reconstruction-induced ordering^{16–17} show that at typical growth temperatures, the maximum $\eta(x, T)$ is $\sim 60\%$. Ordering can exist even at $x = 1/2$, but η is bound by $\eta = \min [2x, 2(1-x)]$, so ordering is maximal at $x = 1/2$. The degree η of LRO is most directly measured by thin-film x-ray diffraction [seeking (1/2, 1/2, 1/2), (1/2, 1/2, -3/2), and (1/2, 1/2, 5/2) zincblende-forbidden reflections] but is more commonly assessed by the less direct approach of modeling of the dynamic transmission-electron-diffraction pattern.²¹ It is also possible to deduce η by fitting to theory the observed nuclear-magnetic-resonance electric-field gradient²² (yielding $\eta \sim 0.6$ in GaInP), the photoluminescence (PL) polarization ratio^{23–24} ($\eta \sim 0.6$), or the crystal-field splitting and bandgap narrowing measured in PL excitation spectra²⁵ ($\eta \leq 0.6$). Such experiments will be reviewed in the following.

It was known for a long time (see review in Reference 18) that samples produced by different growth conditions also exhibit different magnitudes of the physical properties P (such as those listed in the preceding sentence). It was later proven²⁶ that a general relation exists between a physical property $P(\eta)$ for alloys with partial long-range order, and the properties $P(\eta = 0)$ and $P(\eta = 1)$ of the perfectly random and the perfectly ordered cases, respectively:

$$P(\eta) = P(0) + \eta^2[P(1) - P(0)] + O(\eta^4). \quad (3)$$

This relationship opened the door to systematizing various measured properties $P(\eta)$ of samples grown in different ways in terms of their underlying degree η of LRO. Thus a link between growth conditions and degree of ordering could be established.²⁶ This link however requires knowledge of $P(1)$ and $P(0)$. While $P(0)$ can sometimes be measured (e.g., LPE

samples tend to be random), $\eta \equiv 1$ is not attainable experimentally, so $P(1)$ has to be *calculated*. Theoretical calculations of various properties $P(1)$ of ordered compounds (see the following discussion) and experimental measurements of $P(\eta < 1)$ have thus set the stage for useful interplay between experiment and theory through Equation 3.

Naturally the fundamental reason for the difference between $P(0)$ and $P(1)$ ("ordering-induced effects") is the altered symmetry attendant upon ordering. The unit cell of CuPt is twice as large as the zinc-blende unit cell, so its Brillouin zone²³ is halved. Consequently two electronic band-structure states (each characterized by its wave vector \mathbf{k} in the zinc-blende Brillouin zone fold into a single \bar{K} point in the CuPt Brillouin zone. Since CuPt is a (111) superlattice (Figure 1), the zinc-blende L and Γ band-structure states both fold to the CuPt $\bar{\Gamma}$ state. The symmetry of the CuPt $\bar{\Gamma}$ state is thus reduced from T_d in zinc blende to C_{3v} . Hence the threefold degenerate (neglecting spin orbit) top of valence band Γ_{15v} state in zinc blende splits into $\bar{\Gamma}_{3v} + \bar{\Gamma}_{1v}$ ("crystal-field splitting"). The zinc-blende conduction-band minimum now appears as a doublet: the original $\bar{\Gamma}_{1c}^{(1)}(\Gamma_{1c})$ and the folded-in $\bar{\Gamma}_{1c}^{(2)}(L_{1c})$ state. If spin orbit is included, the valence band splits into $E_1 = \bar{\Gamma}_{4,5v}$, $E_2 = \bar{\Gamma}_{6v}^{(1)}$, and $E_3 = \bar{\Gamma}_{6v}^{(2)}$, while the conduction bands are $\bar{\Gamma}_{6c}^{(1)}$ and $\bar{\Gamma}_{6c}^{(2)}$. The relevance of these symmetry labels (subscripts above) becomes clear when one realizes that upon introduction of a perturbation (ordering), states *with the same symmetry* representation anticross—that is, they repel each other (in inverse proportion to their original energy difference and in direct proportion to the perturbation). We will see next that many of the ordering-induced spectroscopic signatures can be simply understood in terms of such "level repulsion."

Bandgap Reduction and Indirect to Direct Crossover

Perhaps the earliest observed fingerprint of ordering in GaInP was the bandgap reduction.¹¹ Kondow et al.²⁷ realized that CuPt ordering leads to L-point folding and computed the band structure in a tight-binding approximation. However they did not note in this calculation any bandgap reduction or crystal-field splitting, presumably since in their calculation atoms were assumed to be tetrahedrally coordinated in the exact zinc-blende structure. Self-consistent first-principle band-structure calculations²⁸⁻²⁹ have revealed that the two equal-symmetry states $\bar{\Gamma}_{1c}^{(1)}(L_{1c})$ and $\bar{\Gamma}_{1c}^{(2)}(\Gamma_{1c})$ (i.e., the

original Γ_{1c} and the L-folded state) repel each other, causing the lower of the two— $\bar{\Gamma}_{1c}^{(1)}$ —to shift down, thus reducing the bandgap. Bandgap reductions $\Delta E_g(1) = E_g(0) - E_g(1)$ between fully random and fully ordered systems were calculated²⁸⁻²⁹ for most III-V and II-VI ordered alloys. Almost all of these predictions await experimental testing. The calculated $\Delta E_g(1)$ for GaInP₂ was used²³⁻²⁶ in the context of Equation 3 to deduce η from measured $E_g(\eta)$. Calculations have shown that $\Delta E_g(1)$ is substantial, for example, 380 ± 40 meV³⁰ (our best-estimate value) in GaInP₂. According to Equation 3, the observed bandgap reductions²⁵ $E_g(\eta) - E_g(0) = 380\eta^2$ correspond to $\eta \leq 60\%$.

The ordering-induced repulsion of energy levels is sometimes so strong as to lead to the lowering of the $\bar{\Gamma}_{1c}^{(1)}(\Gamma_{1c})$ state *below* the X_{1c} state, thus converting upon ordering an indirect-gap material to a direct-gap material. This was predicted to be the case for CuPt-ordered Al_{0.5}Ga_{0.5}As³¹ and for GaAs_{0.5}P_{0.5}.³² Both systems have indirect bandgaps when random and are predicted to transform into direct-gap materials upon CuPt ordering. These predictions await experimental testing. (Preliminary results³³ suggest that ordered Ga₂AsP is indeed direct.)

Another interesting consequence of the ordering-induced level repulsion is that it could reverse the order of bandgaps of two materials: While *random* Cd_{0.5}Hg_{0.5}Te has a lower gap than random GaAs_{0.5}Sb_{0.5}, upon ordering it is predicted²⁹ that the GaAs_{0.5}Sb_{0.5} will have the lower bandgap, opening the door to interesting far-infrared applications for *ordered* antimonides. Such experiments³⁴ indicate an ordering-induced red shift of the bandgap for antimonide alloys toward the desired 8–10- μ m range.

Inverted Band Alignment

Ordering could change a type-I band alignment to type-II band alignment. The ordering-induced repulsion between the conduction bands $\bar{\Gamma}_{1c}^{(1)}(\Gamma_{1c})$ and $\bar{\Gamma}_{1c}^{(2)}(L_{1c})$ lowers the former (the conduction-band minimum [CBM] of the ordered material) relative to the CBM of the random alloy or any reference material (e.g., substrate). The predicted³⁵ conduction-band offset ΔE_c between GaAs and *random* Ga_{0.5}In_{0.5}P is +120 meV (type-I alignment, minimum on GaAs), but ordering is predicted to lower the GaInP₂ CBM by 280 meV, leading to an *inverted* (type II, minimum on GaInP) offset of –160 meV between GaAs and (fully) ordered GaInP₂.

The transition from type-I to type-II band alignment is predicted to occur (for abrupt interfaces) around $\eta = 70\%$. Recent measurements³⁶ indeed find that ΔE_c is reduced by ordering, but the I/II transition is yet to be observed.

The ordering-induced depression of the CBM also leads to the predicted³⁵ formation of a homojunction quantum well between ordered GaInP and disordered GaInP, with both holes ($\Delta E_v \leq 100$ meV) and electrons ($\Delta E_c \leq 250$ meV) in the ordered layer. Such disordered-ordered-disordered structures were recently fabricated,³⁷ and promise to be the basis for interesting devices.

Valence-Band Splitting, Light Polarization, and Spin Polarization

Ordering leads to polarized interband transitions.²³ Either (001) biaxial strain or (111) ordering shift and split the zinc-blende states near the valence-band maximum. Relative to the quantity $\bar{E} = 1/6(\Delta^{SO} + \Delta^{CF})$, the energies are

$$E_1 = 1/2(\Delta^{SO} + \Delta^{CF}),$$

$$E_2 = \frac{1}{2} \sqrt{(\Delta^{SO} + \Delta^{CF})^2 - \frac{8}{3} \Delta^{SO} \Delta^{CF}},$$

and

$$E_3 = -\frac{1}{2} \sqrt{(\Delta^{SO} + \Delta^{CF})^2 - \frac{8}{3} \Delta^{SO} \Delta^{CF}} \quad (4)$$

where Δ^{SO} is the spin-orbit splitting in the absence of crystal-field splitting Δ^{CF} and Δ^{CF} is the crystal-field splitting in the absence of spin-orbit coupling. The difference between strain and ordering is the physical source of Δ^{CF} :

- In the case of *biaxial strain* ε in a zinc-blende material, the physical source of $\Delta^{CF}(\varepsilon)$ is the strain-deformation potential, and the states E_1 , E_2 , and E_3 are, respectively, the heavy-hole Γ_{6v} , the light-hole Γ_{7v} , and the split-off states Γ_{7v} . The transition intensities to the Γ_{6c} conduction band do not depend on the polarization angle in the (001) plane but could depend on the strain ε .

- In the case of *CuPt ordering*, the physical source of $\Delta^{CF}(\eta)$ is the L-folding of *valence-band* states into $\bar{\Gamma}$. This causes level repulsion between the original $\bar{\Gamma}_{3v}(\Gamma_{15})$ valence band and the L-folded $\bar{\Gamma}_{3v}(L_{3v})$. The crystal-field splitting at $\eta = 1$ can be as large as 160 meV (our best estimate) in³⁰ GaInP₂. The interpretation of E_1 , E_2 , and E_3 is now different than from the strain case. Now these states are $\bar{\Gamma}_{4,5v}$, $\bar{\Gamma}_{6v}^{(1)}$ and $\bar{\Gamma}_{6v}^{(2)}$, respectively. The transition intensity $I(\bar{\Gamma}_{4,5v} \rightarrow \bar{\Gamma}_{6c})$ is η -independent, always peaking at

$\theta = [\bar{1}10]$. On the other hand, the two transition intensities $I(\bar{\Gamma}_{6v}^{(1,2)} \rightarrow \bar{\Gamma}_{6c})$ depend on η . Thus they have a nontrivial dependence on polarization angle θ .

These polarization dependences were seen^{24,25} in PL, PLE, and reflectivity, and recently in reflectance difference spectroscopy³⁸ (RDS). The reason for the η -dependence of the intensity is the coupling of $\bar{\Gamma}_{6v}^{(1)}$ with $\bar{\Gamma}_{6v}^{(2)}$. This coupling leads to a *nonlinear* dependence³⁹ of the peak RDS signal on η (missed in the simpler approximation of Reference 38), a dependence that can be used to deduce η from RDS measurements.³⁸ The dependence of polarization intensity on η was also exploited^{23,24} to deduce η directly from fitting the measured $\bar{\Gamma}_{6v}^{(1)} \rightarrow \bar{\Gamma}_{6c}$ intensity to theory.²³ There is an independent way to deduce η from energetic splitting, rather than from polarization intensities: By applying Equation 3 to $\Delta^{SO}(\eta)$ and $\Delta^{CF}(\eta)$ of Equation 4, one can readily calculate the valence-band splitting $E_1 - E_2 = \Delta E_2(\eta)$ versus η . Comparison with the *measured* splitting provides η of this sample^{25,26} [if $\Delta^{CF}(1)$ and $\Delta^{SO}(1)$ are known from calculations]. This valence-field splitting-deduced η ^{25,26} compares very well with η deduced from the polarization intensity,^{23,24} or from that obtained in fitting the calculated bandgap reduction to measurements^{25,26} or from measuring the electric-field gradient in NMR²² (all around $\eta \sim 60\%$). This internal consistency lends some support to our spectroscopic model of ordering, though a direct, model-free measurement of η via x-ray diffraction will be reassuring.

The large $E_1 - E_2$ valence-band splittings attendant upon ordering and the concomitant *polarization*-dependent intensity open the way for using ordered materials as *polarization detectors*. Polarized laser action was also noted from ordered material. Furthermore it has been predicted²³ that photoionization for the $\bar{\Gamma}_{45v}$ state of a single variant ordered sample with *circularly* polarized light will produce electrons that are 100% spin polarized. This potential device application awaits experimental testing. Other predicted optical fingerprints of ordering include the following:²³

- *Optical detection of the ordering type:* By measuring the relative transition intensity using linearly polarized light, one can determine the ordering vectors—that is, distinguishing the variants (CuPt_A from CuPt_B). By using circularly polarized light, one can distinguish the ordering subvariant ($\bar{1}11$) from ($1\bar{1}1$).

- *Removal of “bandgap cusp” via ordering:* Measurement of the bandgap versus

composition in a *strained* alloy usually exhibits a cusp at the composition where the valence-band minimum (VBM) switches from light to heavy hole. The presence of ordering is predicted²³ to remove this cusp.

Both predictions await experimental testing.

Electron-Mass Enhancement

Ordering alters carrier-effective masses. Two effects must be taken into account: The first effect is the well-known reduction of the direct bandgap upon ordering, which tends to *decrease* the electron-effective mass M_e^* . The second effect is the ordering-induced coupling between the Γ_{1c} and the folded-in L_{1c} states. The Γ -L coupling causes a mixing of the corresponding wave functions in the ordered CuPt structure. Since the effective mass of the bulk L_{1c} state [projected along the (111) direction] is much larger than the Γ_{1c} effective mass, the Γ -L coupling is expected to *increase* the electron-effective mass. (This effect was missed in simpler, $\mathbf{k} \cdot \mathbf{p}$ calculations.⁴¹) The resulting effective mass depends on a delicate balance between these two competing effects.

Another consequence of CuPt ordering is the *anisotropy* of the electron-effective mass. While the effective-mass tensor of the perfectly random alloy is isotropic, the ordering-induced coupling between conduction and valence bands breaks the symmetry of the CBM, inducing an anisotropy between the effective mass in the ordering direction and the effective mass in the plane orthogonal to the ordering direction. This anisotropy is enhanced by the Γ -L mixing, because the L_{1c} effective mass is larger in the ordering direction than in the perpendicular directions.

Detailed, first-principles calculations⁴⁰ of effective masses versus ordering and orientation in ordered semiconductors have confirmed the expectations just mentioned including *enhancement* of M_e^* . Recent measurements⁴¹ of excitonic masses are consistent with these predictions, contradicting earlier $\mathbf{k} \cdot \mathbf{p}$ models (predicting *reduction* of M_e^*).

Increase in Critical Pressure for Γ/X Transitions

Pressure converts direct-gap III-Vs (e.g., InP, GaAs, Ga_{0.5}In_{0.5}P) into indirect-gap materials. The bandgap pressure coefficients (derivative of gap with pressure) of ordered and disordered Ga_{0.5}In_{0.5}P alloys have been recently measured by several groups.⁴² These experiments demonstrate that the pressure coefficient

decreases upon ordering. Together with the ordering-induced bandgap reduction, this effect causes a significant *increase* of the critical pressure for the direct-to-indirect (Γ/X) transition with respect to the disordered alloy.

The bandgap pressure coefficient has been calculated⁴³ directly from local-density-approximation (LDA) first-principles band theory. Due to the Γ -L mixing of the CBM wave function, the LDA calculation predicts a *reduction* of the bandgap pressure coefficient from $a = 8.4$ meV/kbar in the disordered alloy ($\eta = 0$) to $a = 6.6$ meV/kbar in the fully ordered CuPt structure ($\eta = 1$). The results for partial degree of order are in good agreement with recent experimental results.⁴² Using LDA-corrected bandgaps, it is estimated that the critical pressure for the Γ -X crossover is 28 kbar in the disordered alloy (in agreement with the experimental results⁴²) and 43 kbar in the ordered CuPt structure. This prediction awaits experimental testing.

Ordering-Induced Electric Fields

An intriguing consequence of the lower symmetry for the CuPt structure is the possibility³⁵ of macroscopic electric polarization since ordering in the CuPt form has a (111) piezoelectric axis. A self-consistent calculation of the electrostatic potential at the interface between CuPt-ordered ($\eta = 1$) GaInP₂ and disordered zinc blende shows an electric field of -9 mV/Å in the (001) direction, originating from the ordered region. For $\eta \sim 0.5$, expect a field that is η^2 times smaller (Equation 3).¹⁶ Free carriers and local microstructural inhomogeneities could further reduce the field. The origin of the electric field is similar to that predicted and later confirmed to exist in artificially grown (111) strained-layer superlattices: Piezoelectric fields generated by the strain in each layer produce a total electric field that has an oscillating component (that varies from layer to layer) and an average component. For a macroscopic superlattice, the average component must be canceled by surface charges. For a thin slice of a superlattice embedded in another material, however, the average field may be nonzero. The piezoelectric fields in GaP and InP are estimated at -3.5 mV/Å and -2.6 mV/Å—that is, smaller than in GaInP₂. If the microstructure of actual samples does not significantly depolarize the field, one would expect important consequences, such as spatial separation of electrons from holes. Current experiments⁴⁴ show internal electric fields that could affect the interpreta-

tion of carrier transport in such material. However the magnitude of such fields is currently uncertain.

Emission at (Much) Higher Energy Than the Absorption Energy

Another exciting consequence of ordering is the appearance of *low-temperature* "up-conversion" from a GaAs/(ordered alloy) system.⁴⁵ One observes emission from the ordered alloy at an energy that is (up to 700 meV) higher than that of the excitation source, even at low temperature where thermal population effects are negligible. Up-conversion was observed⁴⁵ in GaAs/GaInP and GaAs/AlGaInP. The effect was shown to occur when the alloy is ordered. The intensity of the up-converted signal varies super-linearly with excitation density; the up-converted signal disappears when the excitation energy is below the bandgap of GaAs.

The mechanism for up-conversion is not understood. It could be⁴⁵ a cold Auger process (a two-beam experiment⁴⁵ suggests that it is not due to a consecutive, two-step absorption). Since upconversion is seen also in systems where the CBM (VBM) of the alloy is above (below) that of GaAs (type I offset), an essential element of understanding the process is to find out why the up-converted electron and hole recombine in the ordered material rather than diffuse into GaAs. Driessen et al.⁴⁵ suggest that this is due to carrier localization. A natural mechanism⁴⁵ is local clustering, predicted⁴⁶ to lead to both hole and electron localization in GaInP but to localization of only holes in AlInAs and to no localization at all in AlGaAs. This is consistent with the fact that as ordered layers, AlInAs and AlGaAs show no up-conversion. It is possible that local fluctuations in the ordered layer cause carrier localization. Clearly this important and exciting consequence of ordering requires further studies.

Historical Note

Eighty-seven years after Thiel and Koelsch⁴⁷ synthesized the first III-V compound (InP), 68 years after it was determined by Goldschmidt⁴⁸ that the III-Vs have the zinc-blende structure, and 42 years after Goryunova and Fedorova⁴⁹ first succeeded in making the first solid solution of III-V zinc-blende compounds, we have a new type of ordered crystal structure (CuPt) in the III-V alloy family, with new and exciting physics, chemistry, and perhaps, applications.

Acknowledgments

I am grateful to my collaborators, J. Bernard, R. Dandrea, L.G. Ferreira, A. Franceschetti, S. Froyen, D. Laks, J.L. Martins, A. Mascarenhas, G.P. Srivastava, S-H. Wei, and S.B. Zhang. This work was supported by the Department of Energy's (DOE) Office of Energy Research, Basic Energy Science Division of Materials Science, and by the DOE's Energy Efficiency and Renewable Energy Network, under Contract No. DE-AC36-83-CH10093.

References

- J.C. Woolley, in *Compound Semiconductors*, edited by R.K. Willardson and H.L. Goering (Reinhold, New York, 1962) p. 3.
- M.B. Panish and M. Ilegems, in *Progress in Solid State Chemistry*, edited by M. Reiss and J.O. McCaldin (Pergamon Press, New York, 1972) p. 39.
- G.B. Stringfellow, *J. Cryst. Growth* **27** (1974) p. 21; L.M. Foster, *J. Electrochem. Soc.* **121** (1976) p. 1662.
- J.L. Martins and A. Zunger, *Phys. Rev. Lett.* **56** (1986) p. 1400.
- G.P. Srivastava, J.L. Martins, and A. Zunger, *Phys. Rev. B* **31** (1985) p. 2561.
- A. Mbaye, L.G. Ferreira, and A. Zunger, *Phys. Rev. Lett.* **58** (1987) p. 49.
- T.S. Kuan, T.F. Kuech, W.I. Wang, and E.L. Wilkie, *ibid.* **54** (1985) p. 201.
- H. Nakayama and H. Fujita, *Inst. Phys. Conf. Ser.* **79** (1986) p. 289.
- H.R. Jen, M.J. Cheng, and G.B. Stringfellow, *Appl. Phys. Lett.* **48** (1986) p. 1603.
- M.A. Shahid, S. Mahajan, D.E. Laughlin, and H.M. Cox, *Phys. Rev. Lett.* **58** (1987) p. 2567.
- A. Gomyo, T. Suzuki, and S. Iijima, *ibid.* **60** (1988) p. 2645.
- A. Gomyo, K. Makita, I. Hino, and T. Suzuki, *ibid.* **72** (1994) p. 673.
- S-H. Wei, L.G. Ferreira, and A. Zunger, *Phys. Rev. B* **41** (1990) p. 8240.
- R.G. Dandrea, J.E. Bernard, S-H. Wei, and A. Zunger, *Phys. Rev. Lett.* **64** (1990) p. 36.
- S. Froyen and A. Zunger, *ibid.* **66** (1991) p. 2132.
- Ibid.*, *Phys. Rev. B* **53** (1996) p. 4570.
- S.B. Zhang, S. Froyen, and A. Zunger, *Appl. Phys. Lett.* **67** (1995) p. 3141.
- A. Zunger and S. Mahajan, "Atomic Ordering and Phase Separation in Epitaxial III-V Alloys," in *Handbook of Semiconductors*, vol. 3, edited by T.S. Moss (Elsevier Science B.V., Amsterdam, 1994) p. 1399.
- J.R. Smith and A. Zangwill, *Phys. Rev. Lett.* **76** (1996) p. 2097.
- M. Ishimaru, S. Matsumura, N. Kuwano, and K. Oki, *Phys. Rev. B* **51** (1995) p. 9707.
- M.M. Bode, S.P. Ahrenkiel, S.R. Kurtz, K.A. Bertness, D.J. Arent, and J. Olson, in *Optoelectronic Materials—Ordering, Composition Modulation, and Self-Assembled Structures*, edited by E.D. Jones, A. Mascarenhas, P. Petroff, and R. Bhat (Mater. Res. Soc. Symp. Proc. **417**, Pittsburgh, 1996) p. 55.
- D. Mao, P.C. Taylor, S.R. Kurtz, M.C. Wu, and W.A. Harrison, *Phys. Rev. Lett.* **76** (1996) p. 4769; S-H. Wei and A. Zunger, *J. Chem Phys.*

(in press).

- S-H. Wei and A. Zunger, *Phys. Rev. B* **49** (1994) p. 14337.
- T. Kanata, M. Nishimoto, H. Nakayama, and T. Nishino, *Appl. Phys. Lett.* **63** (1993) p. 26.
- P. Ernst, C. Geng, F. Scholz, H. Schwizer, Y. Zhang, and A. Mascarenhas, *ibid.* **67** (1996) p. 2347.
- D.B. Laks, S-H. Wei, and A. Zunger, *Phys. Rev. Lett.* **69** (1992) p. 3766; *Appl. Phys. Lett.* **62** (1993) p. 1937.
- M. Kondow, H. Kakibayashi, S. Minagawa, Y. Inoue, T. Nishino, and Y. Hamakawa, *J. Cryst. Growth* **93** (1988) p. 412.
- A. Zunger, S-H. Wei, L.G. Ferreira, and J.E. Bernard, *Phys. Rev. Lett.* **65** (1990) p. 353.
- S-H. Wei and A. Zunger, *Appl. Phys. Lett.* **56** (1990) p. 662.
- S-H. Wei, A. Franceschetti, and A. Zunger, in *Optoelectronic Materials—Ordering, Composition Modulation, and Self-Assembled Structures*, edited by E.D. Jones, A. Mascarenhas, P. Petroff, and R. Bhat (Mater. Res. Soc. Symp. Proc. **417**, Pittsburgh, 1996) p. 3.
- S-H. Wei and A. Zunger, *Appl. Phys. Lett.* **53** (1988) p. 2077.
- R.G. Dandrea and A. Zunger, *ibid.* **57** (1990) p. 1031.
- T. Takanoashi and M. Ozeki, *Jpn. J. Appl. Phys.* **30** (1991) p. L956.
- S.R. Kurtz, L.R. Dawson, R.M. Biefeld, D.M. Follstaedt, and B.L. Doyle, *Phys. Rev. B* **46** (1992) p. 1909.
- S. Froyen, A. Zunger, and A. Mascarenhas, *Appl. Phys. Lett.* **68** (1996) p. 2852.
- J.J. O'Shea, C.M. Reaves, S.P. DenBaars, M.A. Chin, and V. Narayamurti, *ibid.* **69** (1996) p. 3022.
- R.P. Schneider, E.D. Jones, and D.M. Follstaedt, *ibid.* (1994) p. 587.
- J.S. Luo, J.M. Olson, K. Bertness, M.E. Raikh, and E.V. Tsiper, *J. Vac. Sci. Technol. B* **12** (1994) p. 2552.
- S-H. Wei and A. Zunger, *Phys. Rev. B* **51** (1995) p. 14110.
- A. Franceschetti, S-H. Wei, and A. Zunger, *ibid.* **52** (1995) p. 13992.
- Y. Zhang and A. Mascarenhas, *Phys. Rev. B* **51** (1995) p.13162; E.D. Jones, C. Geng, F. Scholz, and H. Schweizer, *J. Appl. Phys.* **81** (1997) p. 2814.
- R.J. Thomas, H.R. Chandrasekhar, M. Chandrasekhar, E.D. Jones, and R.P. Schneider, *J. Phys. Chem. Solids* **56** (1995) p. 357; references therein.
- A. Franceschetti and A. Zunger, *Appl. Phys. Lett.* **65** (1994) p. 2990.
- P. Ernst, C. Geng, M. Burkard, F. Scholz, and H. Schweizer, *23rd Int. Conf. Phys. Semicond.* (World Scientific, 1996) p. 469.
- F.A.J.M. Driessen, *Appl. Phys. Lett.* **67** (1995) p. 2813; F.A.J.M. Driessen, H.M. Cheong, A. Mascarenhas, S.K. Deb, P.R. Hageman, G.J. Bauhuys, and I.J. Giling, *Phys. Rev. B* **54** (1996) p. 5263.
- K.A. Mader and A. Zunger, *Appl. Phys. Lett.* **74** (1994) p. 2882.
- A. Thiel and H. Koelsch, *Z. Anorg. Allg. Chem.* **66** (1910) p. 288.
- V.M. Goldschmidt, *Trans. Faraday Society* **25** (1929) p. 253.
- N. Goryunova and N. Fedorova, *Zh. Tekh. Fiz.* **25** (1955) p. 1339. □